Scientific Research Publishing

World Journal of Engineering and Technology, 2023, 11, 1019-1029
https://www.scirp.org/journal/wjet
ISSN Online: 2331-4249
ISSN Print: 2331-4222

Significance of Nanoparticles Aggregation with Cattaneo-Christov Heat Flux on the Water and Ethylene Glycol Mixture Based MWCNTs-Nanofluid Flow over a Stretching Cylinder

Muhammad Ramzan*, Nazia Shahmir

Department of Computer Science, Bahria University, Islamabad, Pakistan
Email: *mramzan@bahria.edu.pk

How to cite this paper: Ramzan, M. and Shahmir, N. (2023) Significance of Nanoparticles Aggregation with Cattaneo-Christov Heat Flux on the Water and Ethylene Glycol Mixture Based MWCNTs-Nanofluid Flow over a Stretching Cylinder. *World Journal of Engineering and Technology*, **11**, 1019-1029.
https://doi.org/10.4236/wjet.2023.114068

Received: October 22, 2023
Accepted: November 27, 2023
Published: November 30, 2023

Abstract

This work aims to analyze the flow of electrically conducting MWCNTs-nanofluid over a stretching cylinder with the aggregation and non-aggregation effects of nanoparticles. The working fluid comprised a combination of water and ethylene glycol, with volumetric proportions of (50:50) considered. Convective boundary constraints and modified Fourier law are implemented in heat transmission assessment. The mathematical flow model is formulated in the form of PDEs and is transformed into ODEs via similarity transformation. Numerical outcomes will be obtained with the use of the bvp4c technique and will be displayed with the help of graphs and tables. The results show that the surface drag coefficient is enhanced in the case of aggregation of nanoparticles whereas heat transfer rate is enhanced in the non-aggregation effect of nanoparticles. Furthermore, the temperature distribution enhances the increasing values of particle volume fraction in the case of aggregation effects of nanoparticles whereas temperature distribution lowers in the case of non-aggregation effect of nanoparticles.

Keywords

MWCNTs-Nanofluid, Nanoparticles Aggregation, Water + Ethylene Glycol Mixture, Cattaneo-Christov Heat Flux, Stretching Cylinder

1. Introduction

In recent eras, there has been a quest to achieve remarkable enhancements in

thermal efficiency by utilizing innovative fluid types known as nanofluids. These nanofluids can be described as colloidal solvents that incorporate nanometer-sized particles dispersed within them. These fluid types have experienced remarkable advancements in their practical applications, finding extensive usage in various fields such as refrigeration and air conditioning, transportation, solar thermal systems, microelectronics, mobile computer processors, and high-capacity military communication devices, among others. Their growth in these areas has been unprecedented. Among the various nanoparticles that have been utilized, carbon nanotubes (CNTs) have garnered significant attention from both the scientific and industrial communities worldwide since their groundbreaking discovery. Their unique properties have sparked interest and exploration across a wide range of fields. Subsequently, numerous researchers have integrated carbon nanotubes (CNTs) with various base liquids, forming nanofluids that have been studied in the context of fluid flow over diverse geometries. Sarfaraz and Khan [1] examined the significance of ethylene glycol-based CNT nanofluid flow over a bidirectional extending surface. The numerical estimates of the temperature gradient are shown to be diminishing for the convective dissipation effect. Khan *et al.* [2] obtained the analytical solution of the unsteady CNTs nanofluid flow across two gyrating disks. The temperature distribution is assumed to be more accurate the stronger the values of the unsteadiness parameter. Alzahrani and Khan [3] worked on the intelligent nano-coating simulation for the convective Single-Multi walled carbon nanotubes under the consequences of quadratic drag force and magnetic dipole. The results demonstrate that working liquid particle velocity diminishes as the ferromagnetic interaction parameter improves. Alharbi *et al.* [4] scrutinized the comparative appraisal of carbon nanotubes-based mono and hybrid nanofluid flows due to a three-dimensional surface influence by prescribed temperatures. The important finding showed that in both the PST and PHF case scenarios, the fluid temperature elevates. By using electrically Casson carbon nanotube nanofluid flow in an asymmetrical channel, Noranuar *et al.* [5] investigate heat and mass transmission. The temperature and velocity are greatly improved when the volume percentage of nanoparticles is enhanced.

Various physical phenomena influence the dispersion of nanoparticles (NPs) in a working fluid, consequently impacting the behavior of NPs in the suspension and the properties of nanoparticle fluids (NFs). Among these physical factors, NP aggregation plays a significant role in suspension. Nanoparticle aggregation significantly affects the thermal and rheological characteristics of materials. The aggregated particles often form linear chains [6], which results in the construction of a passageway with a decreased heat resistance. Heat may therefore be transferred through the clusters of nanoparticles extremely fast. The heat conductivity of the nanofluid can be increased in addition to the larger effect volume of aggregations compared to that of nanoparticles [7]. Due to this intrinsic property, researchers have considered the impacts of aggregation for var-

ious nanoparticles over distinct geometries. Wang *et al.*'s [8] investigation focused on the effects of homogeneous and heterogeneous nanoparticle aggregation on the heat radiation-induced flow of titanium dioxide-based nanoliquid across a spinning disk. The study underlines that mass transfer is stronger in fluid flow under aggregation circumstances for enhanced levels of homogeneous and heterogeneous reaction parameters. Zeb *et al.* [9] examined the aggregation effects of magnetic nanoparticles across two rotating disks in a spongy media. Rehman *et al.* [10] numerically analyzed the aggregation impacts on water-based-MWCNTs nanofluid flow along a wedge with irreversibility effects. It is discovered that the entropy production is lower in the nanoparticle aggregation scenario.

It is inferred from the above-cited literature that abundant studies may be found that discuss the nanoparticle aggregation effect on nanofluid flows. But no work is done with the MWCNTs nanoparticles aggregation effects in the binary mixture of water and ethylene glycol. However, the literature has yet to address the flow of MWCNTs-nanofluid with the nanoparticle aggregation effects along an extending cylinder with convective boundary constraints and a modified Fourier equation. The bvp4c function of MATLAB is used to solve the ODEs. Through graphical and tabular demonstrations, the parameters arising in the model are examined in comparison to related profiles.

2. Equations

The mathematical flow model that is being examined involves the incompressible flow of electrically conducting MWCNTs-nanofluid across a stretched cylinder with the influence of nanoparticle aggregation. We consider the binary mixture of water and ethylene glycol as a base fluid. The Z- and R- axes of the cylindrical surface are considered in the horizontal and vertical directions respectively with cylinder radius d as shown in **Figure 1**. The magnetic field strength β_o is employed perpendicular to the Z-axis, whereas at $R \to \infty$ the temperature of the working fluid is maintained at T_∞.

$$\frac{\partial U}{\partial R} + \frac{U}{R} + \frac{\partial W}{\partial Z} = 0, \tag{1}$$

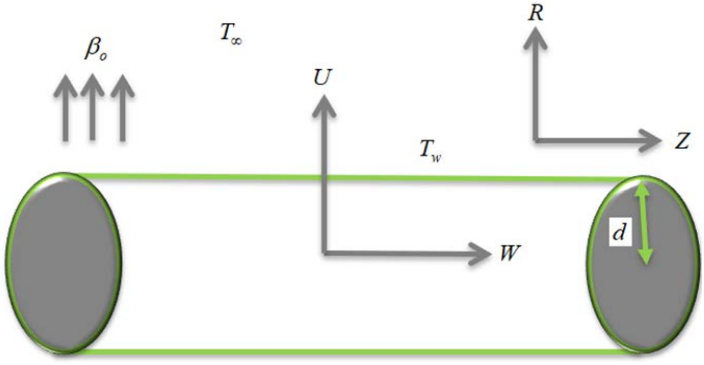

Figure 1. Schematic of the flow model.

$$\rho_{mnf}\left(U\frac{\partial W}{\partial R}+W\frac{\partial W}{\partial Z}\right)=\mu_{mnf}\left(\frac{\partial^2 W}{\partial R^2}+\frac{1}{R}\frac{\partial W}{\partial R}\right)-\frac{\mu_{mnf}}{\bar{k}}W-\sigma_{mnf}\beta_o^2 W, \tag{2}$$

$$\begin{aligned}&\left(\rho c_p\right)_{mnf}\left(W\frac{\partial T}{\partial Z}+U\frac{\partial T}{\partial R}\right)=k_{mnf}\left(\frac{\partial^2 T}{\partial R^2}+\frac{\partial T}{\partial R}\frac{1}{R}\right)+\bar{Q}\left(T-T_\infty\right)\\&-\bar{\lambda}\left(\rho c_p\right)_{mnf}\left(W^2\frac{\partial^2 T}{\partial Z^2}+U^2\frac{\partial^2 T}{\partial R^2}+W\frac{\partial W}{\partial Z}\frac{\partial T}{\partial Z}+2UW\frac{\partial^2 T}{\partial Z\partial R}\right.\\&\left.+W\frac{\partial U}{\partial Z}\frac{\partial T}{\partial R}+U\frac{\partial U}{\partial R}\frac{\partial T}{\partial R}+U\frac{\partial W}{\partial R}\frac{\partial T}{\partial Z}+U\frac{\partial U}{\partial Z}\frac{\partial T}{\partial Z}\right),\end{aligned} \tag{3}$$

with boundary constraints:

$$\begin{gathered}U=0,\ W=w_s,\ -k_{mnf}\frac{\partial T}{\partial R}=h_s\left(T_w-T\right),\quad R=d,\\W\to 0,\ T\to T_\infty,\qquad R\to\infty.\end{gathered} \tag{4}$$

where the parameters arising in Equations (1)-(4) $T_\infty, T_w, \bar{k}, \beta_o, \bar{Q}, \bar{\lambda}, w_s, h_s, \mu_{mnf}, k_{mnf}, \rho_{mnf}, \left(\rho c_p\right)_{mnf}$ represents the ambient temperature, wall temperature, permeability, magnetic field strength, heat source-sink coefficient, thermal relaxation coefficient, stretching velocity, convective heat transfer coefficient, dynamic viscosity, thermal conductivity, density, specific heat capacity of nanofluid. The thermophysical attributes are listed in **Table 1**.

Where in **Table 2** and **Table 3**, the terms $\Phi_a=\frac{\Phi}{\Phi_{INT}}, \Phi_{INT}=\left(\frac{R_a}{R_s}\right)^{D-3}$ are defined as the volume fraction of the MWCNTs in the aggregate and the volume fraction of the aggregates in water respectively. The value of the ratio is taken as $\frac{R_a}{R_s}=4.41$, and Fractal index $D=2.1$. Furthermore, Φ_m is defined as the maximum particle packing fraction, and its value is taken as $\Phi_m=0.0361$.

$$\rho_a=\rho_f\left(1-\Phi_{INT}\right)+\rho_s\Phi_{INT}, \left(\rho c_p\right)_{mnf}=\left(\rho c_p\right)_f\left(1-\Phi_{INT}\right)+\frac{(\Phi\rho)_{INT}}{\left(\rho c_p\right)_f},$$

$$\begin{aligned}k_a=\frac{k_f}{4}\Bigg[&\left(3\Phi_{INT}-1\right)\frac{k_s}{k_f}+\left\{3\left(1-\Phi_{INT}\right)-1\right\}\\&+\left(\left\{\left(3\Phi_{INT}-1\right)\frac{k_s}{k_f}+\left\{3\left(1-\Phi_{INT}\right)-1\right\}\right\}^2+\frac{8k_s}{k_f}\right)^{1/2}\Bigg]\end{aligned}$$

Table 1. Thermal and physical attributes of working fluid and considered nanoparticles [11] [12].

Base fluid/Nanoparticles	Thermal and physical attributes			
	(ρ)	(c_p)	(k)	(σ)
MWCNTs	1600	796	3000	4.8×10^{-7}
$H_2O + C_2H_6O_2$	1059.68	3468	0.404	5.03×10^{-6}

Table 2. Thermal and physical attributes considering the aggregation effects [13] [14].

Thermal and physical attributes	Aggregation
Dynamic viscosity	$\frac{\mu_{mnf}}{\mu_f}=\left(1-\frac{\Phi_a}{\Phi_m}\right)^{-2.5(\Phi_m)}$
Density	$\frac{\rho_{mnf}}{\rho_f}=(1-\Phi_a)+\frac{(\Phi\rho)_a}{\rho_f}$
Specific-heat capacity	$\frac{(\rho c_p)_{mnf}}{(\rho c_p)_f}=(1-\Phi_a)+\frac{(\Phi\rho c_p)_a}{(\rho c_p)_f}$
Thermal conductivity	$\frac{k_{mnf}}{k_f}=\left(\frac{k_a+2k_f+2\Phi_a(k_a-k_f)}{k_a+2k_f-\Phi_a(k_a-k_f)}\right)$
Electrical conductivity	$\frac{\sigma_{mnf}}{\sigma_f}=1+\left(\frac{3\left(\frac{\sigma_a}{\sigma_f}-1\right)\Phi_a}{\left(\frac{\sigma_a}{\sigma_f}+2\right)-\left(\frac{\sigma_a}{\sigma_f}-1\right)\Phi_a}\right)$

Table 3. Thermal and physical attributes considering the non-aggregation effects [13] [14].

Thermal and physical attributes	Non-aggregation
Dynamic viscosity	$\frac{\mu_{mnf}}{\mu_f}=\frac{1}{(1-\Phi)^{2.5}}$
Density	$\frac{\rho_{mnf}}{\rho_f}=(1-\Phi)+\Phi\frac{\rho_s}{\rho_f}$
Specific-heat capacity	$\frac{(\rho c_p)_{mnf}}{(\rho c_p)_f}=(1-\Phi)+\Phi\frac{(\rho c_p)_s}{(\rho c_p)_f}$
Thermal conductivity	$\frac{k_{mnf}}{k_f}=\left(\frac{k_s+2k_f+2\Phi_s(k_s-k_f)}{k_s+2k_f-\Phi_s(k_s-k_f)}\right)$
Electrical conductivity	$\frac{\sigma_{mnf}}{\sigma_f}=1+\left(\frac{3\left(\frac{\sigma_s}{\sigma_f}-1\right)\Phi}{\left(\frac{\sigma_s}{\sigma_f}+2\right)-\left(\frac{\sigma_s}{\sigma_f}-1\right)\Phi}\right)$

whereas the correlations used above are defined as the density, specific heat capacity, and thermal conductivity of the MWCNTs in the aggregate. The subscripts (*s*) illustrate the solid particle, (*f*) is used for fluid, and (*mnf*) is used for nanofluid.

Following are the similarity transformations used to simplify the system of Equations (1)-(4):

$$U=-\frac{cd}{\sqrt{\xi}}f(\xi),\quad \xi=\left(\frac{R}{d}\right)^2,\quad W=2Zcf'(\xi),\quad \theta(\xi)=\frac{T-T_\infty}{T_w-T_\infty}, \tag{5}$$

With trivially fulfilled continuity Equation (1), Equations (2)-(4) are modified as follows:

$$\left(\frac{\mu_{mnf}}{\rho_{mnf}}\right)(\xi f'''+f'')-\left(\frac{\mu_{mnf}}{\rho_{mnf}}\right)R_o f'-\mathrm{Re}\left(f'^2-ff''\right)-\left(\frac{\sigma_{mnf}}{\rho_{mnf}}\right)Mf'=0, \tag{6}$$

$$\frac{k_{mnf}}{k_f}(\xi\theta''+\theta')+Q_o\theta+\frac{(\rho C_p)_{mnf}}{(\rho C_p)_f}\mathrm{Re}\,\mathrm{Pr}\,\theta' f-2\lambda\,\mathrm{Re}\,\mathrm{Pr}\frac{(\rho C_p)_{mnf}}{(\rho C_p)_f}\left(f^2\theta''+ff'\theta'\right)=0. \tag{7}$$

Cylindrical surface boundary constraints are:

$$f(1)=0,\quad f'(1)=1,\quad -\frac{k_{mnf}}{k_f}\theta'(1)=B_i\left(1+\theta(1)\right),\quad f'(\infty),\quad \theta(\infty). \tag{8}$$

Here, $\xi, R_o, \mathrm{Re}, M, Q_o, \mathrm{Pr}, \lambda$, and B_i illustrated as Similarity variable, porosity parameter, Reynold number, Magnetic parameter, Heat generation parameter, Prandtl number, Thermal relaxation parameter, and Biot number. These are delineated as follows:

$$\mathrm{Re}=\frac{cd^2}{2\nu_f}, M=\frac{\sigma_f\beta_o^2d^2}{4\mu_f}, R_o=\frac{d^2}{4\bar{k}}, Q_o=\frac{\bar{Q}d^2}{4k_f}, \mathrm{Pr}=\frac{\nu_f\left(\rho C_p\right)_f}{\rho_f k_f}, \lambda=\bar{\lambda}c. \tag{9}$$

The expressions for the surface drag coefficient C_f with shear stress τ_s and heat transmission rate N_u with heat flux q_s are:

$$C_f=\frac{2\tau_s}{\rho_{f w_s}^2}, \tau_s=\mu_{mnf}\frac{\partial W}{\partial R}, N_u=\frac{dq_s}{k_f\left(T_w-T_\infty\right)}, q_s=-k_{mnf}\frac{\partial T}{\partial R}. \tag{10}$$

The non-dimensional form of Equation (10) is appended as:

$$C_f\,\mathrm{Re}_z=\frac{\mu_{mnf}}{\mu_f}f''(1), N_u=-2\frac{k_{mnf}}{k_f}\theta'(1). \tag{11}$$

where Re_z is denoted as the local Reynold number.

3. Figures and Numerical Tables

This section featured graphs and tables to present and illustrate the numerical results that the bvp4c scheme produced. **Figure 2** is sketched to display the role of Reynold's number (Re) on the velocity distribution $f'(\xi)$. It is inferred that for mounting estimations of (Re), dwindled the $f'(\xi)$. This dwindling trend is noticed higher when the aggregation of nanoparticles is considered. **Figure 3** depicts the impact of the porosity parameter (R_o) over the velocity distribution $f'(\xi)$. It is noted that the velocity distribution declined against higher values of (R_o). When the aggregation of nanoparticles is considered, this declining capacity becomes more obvious. Furthermore, **Figure 4** is portrayed to visualize the influence of particle volume fraction (Φ) on the temperature distribution $\theta(\xi)$. It is interesting to note that temperature distribution

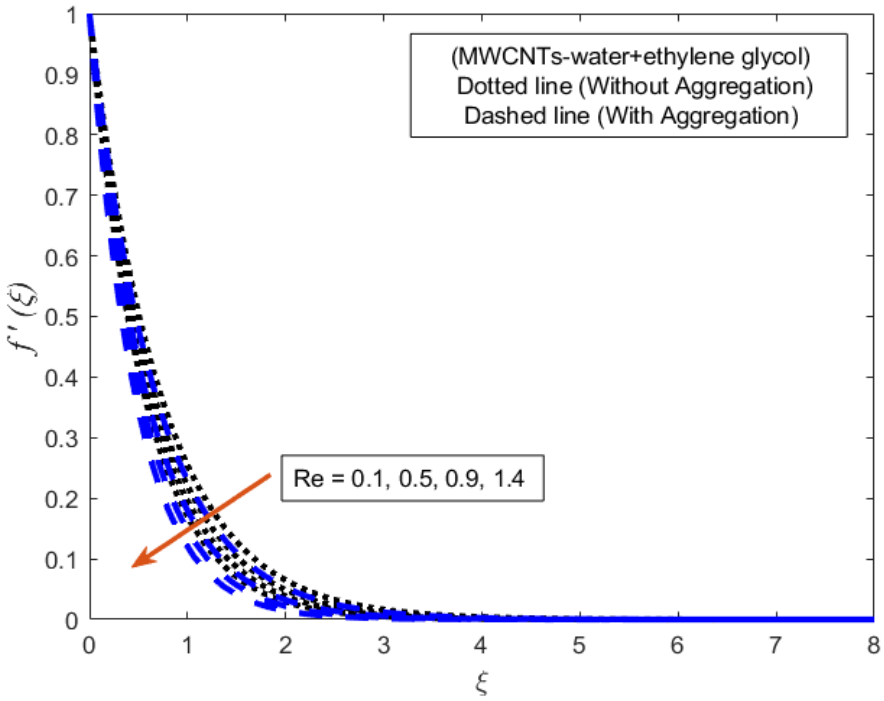

Figure 2. Upshot of Reynold number on the velocity profile.

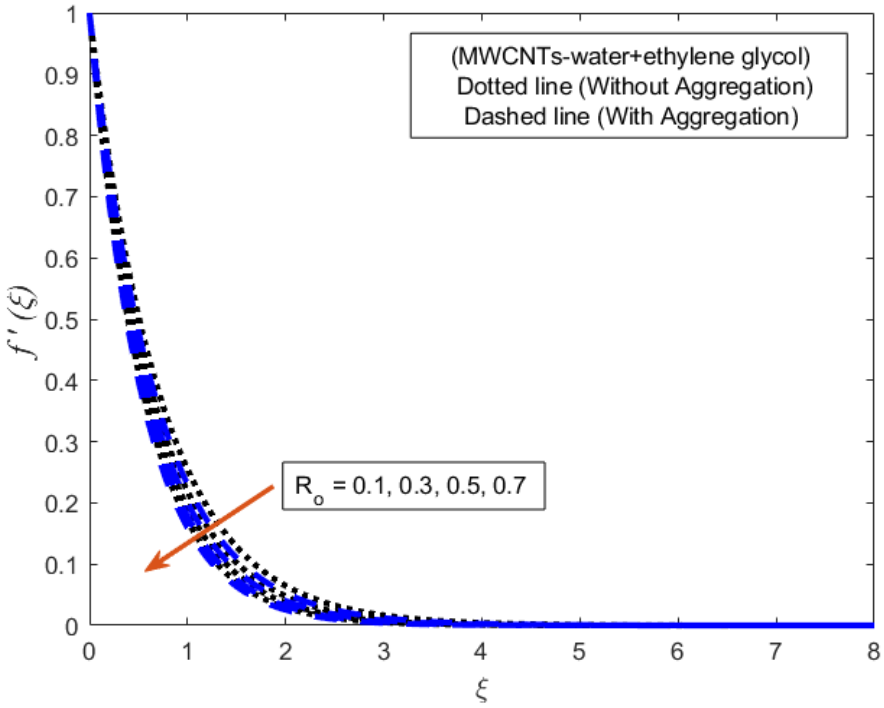

Figure 3. Upshot of porosity parameter on the velocity profile.

$\theta(\xi)$ escalates when the influence of aggregation of nanoparticles is considered whereas it dwindled in the case of non-aggregation of nanoparticles. **Figure 5** is illustrated to show the consequences of the thermal relaxation parameter over the temperature distribution. It is shown that the temperature profile drops for

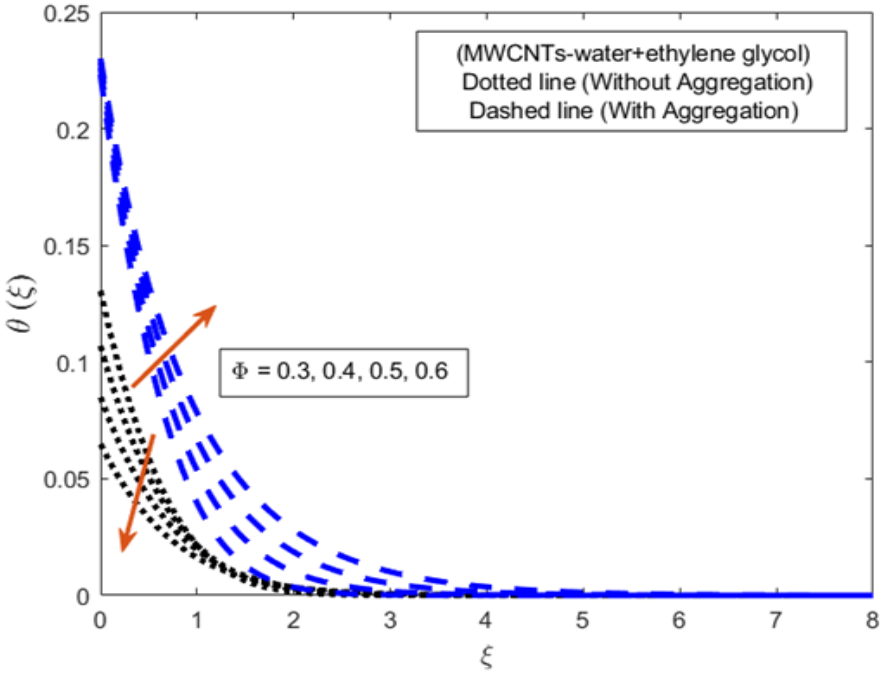

Figure 4. Upshot of Particle volume fraction on the temperature profile.

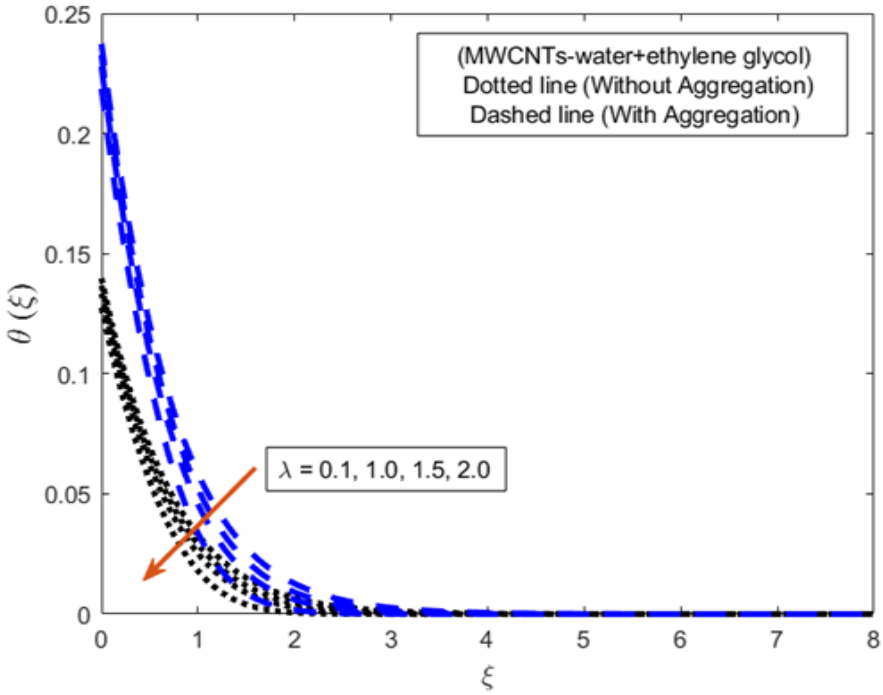

Figure 5. Upshot of thermal relaxation parameter on the temperature profile.

higher estimations of (λ). When the situation of non-aggregation of nanoparticles is taken into consideration, this diminishing tendency becomes more apparent. Next, **Table 4** is tabulated to obtain the numerical estimations of the surface drag coefficient (C_f) for aggregation and non-aggregation effects of nanoparticles for the $(\mathrm{Re}, \Phi_{mnf}, M)$. It is noticed that the surface drag coeffi-

cient reduces more when non-aggregation effects of nanoparticles are considered for greater values of (Re) and (M). **Table 5** is drawn to uncover the impact of $(\mathrm{Re}, \Phi_{mnf}, Q)$ on the heat transfer rate (Nu) for both cases of aggregation and non-aggregation effects of nanoparticles. It is revealed that for higher values of Reynold number (Re) and particles volume fraction (Φ) the heat transfer escalates more significantly when non – aggregation effects of nanoparticles are considered. Furthermore, for the escalating values of heat source/sink parameter (Q) the heat transfer rate dwindled more in the case of aggregation effects of nanoparticles.

Table 4. Numerical values of surface drag coefficient for aggregation and non-aggregation effects.

Re	Φ_{mnf}	M	Aggregation	Non-Aggregation
0.10	0.30	0.10	−1.77518	−3.33865
0.11			−1.78363	−3.34827
0.12			−1.79200	−3.35785
	0.31		−1.78842	−3.45793
	0.32		−1.80178	−3.58344
		0.20	−1.83202	−3.30325
		0.30	−1.88600	−3.30326

Table 5. Numerical estimations of heat transfer rate for aggregation and non-aggregation effects.

Re	Φ_{mnf}	Q	Aggregation	Non-Aggregation
0.10	0.30	0.10	0.388394	0.434693
0.11			0.389791	0.435598
0.12			0.391133	0.436467
	0.31		0.388249	0.435917
	0.32		0.388105	0.437132
		0.15	0.386520	0.434096
		0.20	0.384516	0.433478

4. Conclusions

The following are the most notable findings of this investigation:

- The mounting estimations of Reynold's number dwindled the velocity profile. This dwindling trend is noticed higher when the aggregation of nanoparticles is considered.
- The temperature distribution escalates in the aggregation of nanoparticles whereas it dwindles in the non-aggregation of nanoparticles for the increasing volume fraction.

- The surface drag coefficient reduces more significantly when non-aggregation effects of nanoparticles are considered against Reynold number.
- For higher values of Reynold number and particles volume fraction the heat transmission escalates more significantly when non-aggregation effects of nanoparticles are considered.

Acknowledgments

The study is supported by Bahria University, Islamabad, Pakistan.

Conflicts of Interest

The authors declare no conflicts of interest regarding the publication of this paper.

References

[1] Sarfraz, M. and Khan, M. (2022) Significance of Ethylene Glycol-Based CNT Homann Nanofluid Flow over a Biaxially Stretching Surface. *Waves in Random and Complex Media*, 1-15. https://doi.org/10.1080/17455030.2022.2075048

[2] Khan, S.A., Khan, I., Gul, T., Ullah, I., Rehman, M.U., Ullah, A. and Shah, S.A. (2022) Comparative Analysis of the CNTs Nano Fluid Flow between the Two Gyrating Disks. *Advances in Mechanical Engineering*, **14**, 1-13. https://doi.org/10.1177/16878132221093124

[3] Alzahrani, F. and Khan, M.I. (2022) Analysis of Wu's Slip and CNTs (Single and Multi-Wall Carbon Nanotubes) in Darcy-Forchheimer Mixed Convective Nanofluid Flow with Magnetic Dipole: Intelligent Nano-Coating Simulation. *Materials Science and Engineering: B*, **277**, 115586. https://doi.org/10.1016/j.mseb.2021.115586

[4] Alharbi, K.A.M., Ramzan, M., Shahmir, N., Ghazwani, H.A.S., Elmasry, Y., Eldin, S. M. and Bilal, M. (2023) Comparative Appraisal of Mono and Hybrid Nanofluid Flows Comprising Carbon Nanotubes over a Three-Dimensional Surface Impacted by Cattaneo-Christov Heat Flux. *Scientific Reports*, **13**, Article No. 7964. https://doi.org/10.1038/s41598-023-34686-8

[5] Noranuar, W.N.I.N., Mohamad, A.Q., Shafie, S. and Jiann, L.Y. (2023) Heat and Mass Transfer on Magnetohydrodynamics Casson Carbon Nanotubes Nanofluid Flow in an Asymmetrical Channel via Porous Medium. *Symmetry*, **15**, 946. https://doi.org/10.3390/sym15040946

[6] Murshed, S.M.S., Leong, K.C. and Yang, C. (2005) Enhanced Thermal Conductivity of TiO_2-Water Based Nanofluids. *International Journal of thermal sciences*, **44**, 367-373. https://doi.org/10.1016/j.ijthermalsci.2004.12.005

[7] Prasher, R., Phelan, P.E., and Bhattacharya, P. (2006) Effect of Aggregation Kinetics on the Thermal Conductivity of Nanoscale Colloidal Solutions (Nanofluid). *Nano letters*, **6**, 1529-1534. https://doi.org/10.1016/j.ijthermalsci.2004.12.005

[8] Wang, F., Kumar, R.N., Prasannakumara, B.C., Khan, U., Zaib, A., Abdel-Aty, A.H. and Galal, A.M. (2022) Aspects of Uniform Horizontal Magnetic Field and Nanoparticle Aggregation in the Flow of Nanofluid with Melting Heat Transfer. *Nanomaterials*, **12**, 1000. https://doi.org/10.3390/nano12061000

[9] Zeb, H., Wahab, H.A., Khan, U., Ehab, M. and Malik, M.Y. (2022) The Modified Heat Flux Modeling in Nanoparticles (Fe_3O_4 and Aggregation Nanoparticle) Based Fluid between Two Rotating Disks. *Energies*, **15**, 4088.

https://doi.org/10.3390/en15114088

[10] Rehman, R., Wahab, H.A., Alshammari, N., Khan, U. and Khan, I. (2022) Aggregation Effects on Entropy Generation Analysis for Nanofluid Flow over a Wedge with Thermal Radiation: A Numerical Investigation. *Journal of Nanomaterials*, **2022**, Article ID: 3992590. https://doi.org/10.1155/2022/3992590

[11] Zakaria, I., Azmi, W.H., Mamat, A.M.I., Mamat, R., Saidur, R., Talib, S.F.A. and Mohamed, W.A.N.W. (2016) Single PEM Fuel Cell Cooling Plate: An Experimental Study. *International Journal of Hydrogen Energy*, **41**, 5096-5112. https://doi.org/10.1016/j.ijhydene.2016.01.041

[12] Islam, M.R., Shabani, B. and Rosengarten, G. (2017) Electrical and Thermal Conductivities of 50/50 Water-Ethylene Glycol Based TiO_2 Nanofluids to Be Used as Coolants in PEM Fuel Cells. *Energy Procedia*, **110**, 101-108. https://doi.org/10.1016/j.egypro.2017.03.113

[13] Benos, L.T., Karvelas, E.G. and Sarris, I.E. (2019) Crucial Effect of Aggregations in CNT-Water Nanofluid Magnetohydrodynamic Natural Convection. *Thermal Science and Engineering Progress*, **11**, 263-271. https://doi.org/10.1016/j.tsep.2019.04.007

[14] Wang, F., Rani, S.P., Sarada, K., Gowda, R.P., Zahran, H.Y. and Mahmoud, E.E. (2022) The Effects of Nanoparticle Aggregation and Radiation on the Flow of Nanofluid between the Gap of a Disk and Cone. *Case Studies in Thermal Engineering*, **33**, 101930. https://doi.org/10.1016/j.csite.2022.101930